ISSN 2186-6570

Performance of the Neyman-Pearson Receiver for a Binary Thermal Coherent State Signal

Kentaro Kato

Quantum ICT Research Institute, Tamagawa University
6-1-1 Tamagawa-gakuen, Machida, Tokyo 194-8610, Japan

Tamagawa University Quantum ICT Research Institute Bulletin, Vol.5, No.1, 11-18, 2015

Tamagawa University Quantum ICT Research Institute Bulletin
Vol.5 No.1 : 11–18 (2015)

Performance of the Neyman-Pearson Receiver for a Binary Thermal Coherent State Signal

Kentaro Kato
Quantum Communication Research Center,
Quantum ICT Research Institute, Tamagawa University
6-1-1 Tamagawa-gakuen, Machida, Tokyo 194-8610 Japan
E-mail: kkatop@lab.tamagawa.ac.jp

***Abstract*—The performance of the quantum Neyman-Pearson receiver for a binary coherent state signal in the presence of thermal noise is numerically investigated. To see the detection sensitivity of the quantum Neyman-Pearson receiver, its receiver operating characteristics (ROC) are numerically obtained. The performance limit of the quantum Neyman-Pearson receiver is directly computed when the false alarm probability is very small, and the simulation result of the binary thermal coherent state signal is compared to that of the case of random phase signal.**

I. Introduction

The Neyman-Pearson (NP) criterion was originally developed for binary hypothesis testing [1], [2]. The idea of the NP criterion was applied to optimal signal detection problem in the early days of radar technologies [3], [4]. It is nowadays considered as one of fundamental signal processing techniques for radar systems [5].

The first application of the NP criterion to quantum signal detection was considered by Helstrom [6]. In the literatures [7], [8] the performance of the quantum NP receiver for a binary coherent state signal of random phase is well analyzed in the presence of thermal noise. An analysis for the corresponding non-random phase case was discussed by Yoshitani [9] through a third-order perturbative calculation. However, the analysis is valid only for the case of very small thermal noise due to the perturbative calculation, and hence the performance evaluation for the thermal coherent state signal having non-random phase in wider range of thermal noise exceeding the small noise case is remaining. Therefore, the aim of this paper is to expand beyond the preceding works by focusing on the numerical evaluation of the receiver.

II. Neyman-Pearson criterion in Quantum Detection

Here, we introduce a general approach of the quantum NP criterion in accordance with Helstrom [10]. Suppose that there are two quantum hypotheses, H_0 and H_1, that are associated with two distinct quantum-states $\hat{\rho}_0$ and $\hat{\rho}_1$, respectively, and let $\mathit{\Pi} = (\hat{\Pi}_0, \hat{\Pi}_1) = (\hat{1} - \hat{\Pi}_1, \hat{\Pi}_1)$ denote a positive operator-valued measure (POVM) that describes the mathematical model of a detector. The false alarm of the detection is characterized by

$$Q_0 = \Pr\{\mathsf{H}_1|\mathsf{H}_0\} = \mathrm{Tr}\hat{\Pi}_1\hat{\rho}_0, \tag{1}$$

and the detection probability is defined as

$$Q_\mathrm{d} = 1 - \Pr\{\mathsf{H}_0|\mathsf{H}_1\} = \Pr\{\mathsf{H}_1|\mathsf{H}_1\} = \mathrm{Tr}\hat{\Pi}_1\hat{\rho}_1. \tag{2}$$

The problem is to maximize the detection probability Q_d under the constraint $Q_0 \leq \alpha_0$, where α_0 is a preassigned constant. Using the undetermined multiplier method, the function F to be maximized is written as

$$\begin{aligned} F &= Q_\mathrm{d} - \zeta(Q_0 - \alpha_0) \\ &= \alpha_0\zeta + \mathrm{Tr}\hat{\Pi}_1(\hat{\rho}_1 - \zeta\hat{\rho}_0) \end{aligned} \tag{3}$$

with an undetermined multiplier $\zeta \geq 0$. If the operator $\hat{\rho}_1 - \zeta\hat{\rho}_0$ can be decomposed into the form

$$\hat{\rho}_1 - \zeta\hat{\rho}_0 = \sum_i \lambda_i(\zeta)|\lambda_i(\zeta)\rangle\langle\lambda_i(\zeta)| \tag{4}$$

with its eigenvalues $\lambda_i(\zeta)$ and eigenvectors $|\lambda_i(\zeta)\rangle$, then the detection operator

$$\hat{\Pi}_1(\zeta) = \sum_{i:\lambda_i(\zeta)>0} |\lambda_i(\zeta)\rangle\langle\lambda_i(\zeta)|, \tag{5}$$

maximizes F for a fixed ζ when zero eigenvalues occur from a set of measure zero. Letting

$$\alpha(\zeta) = \sum_{i:\lambda_i(\zeta)>0} \langle\lambda_i(\zeta)|\hat{\rho}_0|\lambda_i(\zeta)\rangle \tag{6}$$

and

$$\beta(\zeta) = 1 - \sum_{i:\lambda_i(\zeta)>0} \langle\lambda_i(\zeta)|\hat{\rho}_1|\lambda_i(\zeta)\rangle, \tag{7}$$

the problem is reduced to finding the optimal ζ that maximizes $1 - \beta(\zeta)$ under the constraint $\alpha(\zeta) \leq \alpha_0$. For this problem, one may use the bisection search (or its variant such as the golden section search) to find the optimal ζ°, because the function $\alpha(\zeta)$ is a monotonically decreasing function of ζ due to the convexity of the set of all possible points (Q_0, Q_d) (*e.g.* Fig.4. See also the region D in Fig.4.2. of the textbook [10]). Therefore, a rough sketch of the calculation procedure for finding the best detection probability $Q_\mathrm{d} = 1 - \beta(\zeta^\circ)$ is given as follows:

1) [α_0 is given]
2) Do the bisection search to find the optimal ζ° under the constraint $\alpha(\zeta) \leq \alpha_0$. In each stage of the bisection search, compute $\alpha(\zeta)$ by using Eq.(6).

3) Once the optimal ζ° is found, compute $Q_{\rm d} = 1 - \beta(\zeta^\circ)$ by using Eq.(7).

This procedure is used to find the best detection probability $Q_{\rm d}$ for our problem in Section IV.

III. Matrix Representation of Thermal Coherent States

Suppose that a binary coherent state signal $\{|0\rangle, |\gamma\rangle\}$ is in the pressure of thermal noise, where $|0\rangle$ is the vacuum state and $|\gamma\rangle$ the coherent state of complex amplitude γ. In this situation, we assume that the received signals are given by the thermal vacuum and thermal coherent states. The density operator of the thermal vacuum is expressed in the following P-representation.

$$\begin{aligned}\hat{\rho}_0 &= \hat{\rho}_{\rm th}(0) \\ &= \frac{1}{\pi n_{\rm th}} \int \exp[-\frac{|\gamma'|^2}{n_{\rm th}}] |\gamma'\rangle\langle\gamma'| {\rm d}^2\gamma', \end{aligned} \quad (8)$$

where $n_{\rm th}$ is the average photon number of thermal noise given by $n_{\rm th} = ({\rm e}^{\hbar\omega/k_{\rm B}T} - 1)^{-1}$ with the angular frequency ω of light, Boltzmann constant $k_{\rm B}$, and the absolute temperature T. This state is also written as

$$\hat{\rho}_0 = (1-\nu)\sum_{n=0}^{\infty} \nu^n |n\rangle\langle n|, \quad (9)$$

where the real parameter ν is defined by $\nu = n_{\rm th}/(1+n_{\rm th})$, or $n_{\rm th} = \nu/(1-\nu)$. On the other hand, the thermal coherent state with complex amplitude γ is given by

$$\begin{aligned}\hat{\rho}_1 &= \hat{\rho}_{\rm th}(\gamma) \\ &= \frac{1}{\pi n_{\rm th}} \int \exp[-\frac{|\gamma' - \gamma|^2}{n_{\rm th}}] |\gamma'\rangle\langle\gamma'| {\rm d}^2\gamma'. \end{aligned} \quad (10)$$

The matrix representation of $\hat{\rho}_1$ in the basis $\{|n\rangle\}$ is given as follows [11]:

$$\begin{aligned}\langle m|\hat{\rho}_1|n\rangle &= \sqrt{\frac{m!}{n!}}(1-\nu)\nu^n \\ &\quad \times \left(\frac{(1-\nu)\gamma^*}{\nu}\right)^{n-m} \\ &\quad \times \exp[-(1-\nu)|\gamma|^2] \\ &\quad \times {\rm L}_m^{(n-m)}[-\frac{(1-\nu)^2|\gamma|^2}{\nu}], \\ &\qquad\qquad \text{if } m \le n, \end{aligned} \quad (11)$$

$$\langle m|\hat{\rho}_1|n\rangle = (\langle n|\hat{\rho}_1|m\rangle)^*, \qquad \text{if } m > n, \quad (12)$$

where ${\rm L}_n^{(m)}[x]$ is the associated Laguerre polynomial ([12], [14]). By using Eq.(9) and Eqs.(11)-(12), one can obtain a matrix representation of $\hat{\rho}_1 - \zeta\hat{\rho}_0$ in the ordered basis $\{|0\rangle, |1\rangle, |2\rangle, \dots\}$. Since a computer can handle only a finite matrix size, one must employ an appropriate cut-off rule for the matrix size. In this study, we have used the same cut-off rule for the matrix size as that of the literature [13]: For a finite size matrix representation $\rho_i = [\langle m|\hat{\rho}_i|n\rangle]_{m=0,1,\dots,D-1}^{n=0,1,\dots,D-1}$ of the state $\hat{\rho}_i$ $(i = 0, 1)$, (i) compute ${\rm Tr}\rho_i$ and ${\rm Tr}\rho_i^2$, (ii) compare them with 1 and $(1-\nu)/(1+\nu)$, respectively, and (iii) check whether the errors are within a preassigned accuracy $\epsilon_{\rm matrix}$.

IV. Performance of the Neyman-Pearson Receiver for Binary Thermal Coherent State Signal

In the detection theory, the receiver operating characteristic (ROC), which indicates the performance of $Q_{\rm d}$ against α_0, is often used to evaluate the detection sensitivity of a receiver. The ROC of the quantum NP receiver for decision between two pure coherent states $|0\rangle$ and $|\gamma\rangle$ is shown in (a) of Fig. 1, where we have assumed γ is real and have set to $\gamma^2 = 0.01, 0.1, 0.5, 1,$ and 2 (See also Appendix). The effect of thermal noise can be observed in (b.1)-(b.5) of Fig. 1, where we have used the following conditions for calculation:

- γ is real;
- $\hat{\rho}_0 = \hat{\rho}_{\rm th}(0)$ and $\hat{\rho}_1 = \hat{\rho}_{\rm th}(\gamma)$;
- $\gamma^2 = 0.01, 0.1, 0.5, 1,$ and 2;
- $n_{\rm th} = 0$, 0.01, 0.1, 1 and 5, or $\nu = 0$, 0.0099, 0.091, 0.5 and 0.83.

The calculation program is based on the procedure mentioned in Section II. The source code of the calculation program was written in C++ and was compiled by Intel compiler on CentOS 5 (x86_64). To compute some special functions and to find the eigenvalues and eigenvectors of a matrix, GNU Scientific Library (GSL) [14] was used. The accuracy $\epsilon_{\rm matrix}$ for determining the matrix size was set to 10^{-13}, so that the number D of the rows (which equals to that of the columns) of the matrix representation ρ_i $(i = 0, 1)$ was determined according to satisfying this accuracy. In each stage of the optimization process for parameter ζ, the eigenvalue problem of $(1/(1+\zeta))\rho_1 - (\zeta/(1+\zeta))\rho_0$ was solved instead of that of $\rho_1 - \zeta\rho_0$. The initial values for the bisection search were set to $\zeta_{\rm lft}^{0)}/(1+\zeta_{\rm lft}^{0)}) = 0.0$ (or $\zeta_{\rm lft}^{0)} = 0$) and $\zeta_{\rm rht}^{0)}/(1+\zeta_{\rm rht}^{0)}) = 0.99999$ (or $\zeta_{\rm rht}^{0)} = 99999.0$), which was chosen heuristically to cover all the case under consideration. Moreover, the accuracy for the bisection search $\epsilon_{\rm search}$ was set to $\epsilon_{\rm search} = 10^{-12}$, that is, the iteration halted when $\zeta_{\rm rht}^{s)} - \zeta_{\rm lft}^{s)} < \epsilon_{\rm search}$ is satisfied at an sth stage. In our simulation, we observed that the resulting ζ° yields $\alpha(\zeta^\circ) = \alpha_0$ within accuracy 10^{-10}. Finally, we numerically checked the completeness of the resulting eigenvectors with accuracy 10^{-12}. It means that every entry of the matrix consisting of the sum of the dyadic product of the resulting eivenvectors is identical to the corresponding entry of the identity matrix within the accuracy 10^{-12}.

As shown in (b-1) to (b-5), we observe the performance degradation of the quantum NP receiver due to the thermal noise in each γ^2. From the comparison of the cases of $\gamma^2 = 0.01$ and $\gamma^2 = 2$, we can find the difference of the speed of the performance degradation against the

increase of the average number $n_{\rm th}$ of photons of thermal noise. In this comparison, the latter might seem to be more degraded against the increase of $n_{\rm th}$ than the former. But, when the average number $n_{\rm th}$ of photons of thermal noise is fixed, the ROC curves are lifted upwards as γ^2 increases. Hence the improvement of the signal-to-noise ratio is essential for the detection sensitivity of the quantum NP receiver.

In radar/lidar applications, the case of small α_0 is of much interest. Fig. 2 shows the detection probability $Q_{\rm d}$ versus γ^2 when α_0 is small. The simulation condition is as follows:

- $\alpha_0 = 10^{-2}, 10^{-4}, 10^{-6}$;
- γ is real, and $0.1 \le \gamma^2 \le 18$;
- $n_{\rm th} = 0$, 0.05, 0.1, 0.5, 1, and 5, or $\nu = 0$, 0.048, 0.091, 0.33, 0.5, and 0.83;

where the computing environment (including the initial set-ups, the verification level of the completeness of the eigenvectors, and so on) is the same as in the case of Fig. 1. From these figures, we see that the behavior of the curves in each figure is similar except its scaling of the probabilities. It can be seen as a reflection of the trade-off between the detection probability $Q_{\rm d}$ and the false-alarm level α_0.

Here we consider the case that the phase of the amplitude γ is uniformly distributed for comparison. In this case the signal state $\hat{\rho}_1$ is replaced to

$$\begin{aligned}\hat{\rho}_1 &= \overline{\hat{\rho}_{\rm th}(|\gamma|{\rm e}^{\varphi})} \\ &= \frac{1}{2\pi}\int_0^{2\pi}\Big[\frac{1}{\pi n_{\rm th}}\int \exp[-\frac{|\gamma'-|\gamma|{\rm e}^{{\rm i}\varphi}|}{n_{\rm th}}] \\ &\qquad \times|\gamma'\rangle\langle\gamma'|{\rm d}^2\gamma'\Big]{\rm d}\varphi \\ &= \frac{1}{\pi n_{\rm th}}\int \exp[-\frac{|\gamma'|^2+|\gamma^2|}{n_{\rm th}}] \\ &\qquad \times{\sf I}_0[\frac{2|\gamma'||\gamma|}{n_{\rm th}}]|\gamma'\rangle\langle\gamma'|{\rm d}^2\gamma', \quad (13)\end{aligned}$$

where ${\sf I}_0[x]$ is the modified Bessel function of order zero ([12], [14], [15]). The detection probability $Q_{\rm d}$ for this random phase signal is given [7] by

$$Q_{\rm d} = 1 - \sum_{n=0}^{z-1} P_{n1} - (1-q)P_{z1}, \quad (14)$$

where the fraction q is determined by $\alpha_0 = q(1-\nu)\nu^z + \nu^{z+1}$ and the decision level $z = \lfloor(\ln\alpha_0)/(\ln\nu)\rfloor$, and

$$\begin{aligned}P_{n0} &= (1-\nu)\nu^n, \quad (15)\\ P_{n1} &= (1-\nu)\nu^n\exp[-(1-\nu)|\gamma^2|] \\ &\qquad \times{\sf L}_n[-(1-\nu)^2|\gamma|^2/\nu], \quad (16)\end{aligned}$$

with the Laguerre polynomial ${\sf L}_n[x]$ ([12], [14]). The detection probability $Q_{\rm d}$ for the case of random phase signal is shown in Fig. 3, together with that for the non-random phase signal. The solid lines are identical to the corresponding $Q_{\rm d}$ shown in Fig. 2, and the dashed lines are obtained from Eq.(14). In each figure, the difference between the detection probabilities of two cases becomes larger as γ^2 increases. The parameter γ^2 can be regarded as a measure of closeness of the two signals. The effect of randomness of the phase clearly appears when the two signals are apart from each other in each case of $n_{\rm th}$. Conversely, it seems to be limited when the signals are closer.

V. CONCLUSION

We considered the quantum Neyman-Pearson receiver for a binary coherent state signal in the presence of thermal noise. The receiver operating characteristic (ROC) curves of the quantum Neyman-Pearson receiver for binary thermal coherent state signal were numerically obtained. The performance limit of the quantum Neyman-Pearson receiver was obtained via direct calculation of the eigenvalues and eigenvectors of the operator $\hat{\rho}_1 - \zeta\hat{\rho}_0$ when the false alarm level $\alpha_0 = 10^{-2}$, 10^{-4}, and 10^{-6}. Further, the simulation result for the binary thermal coherent state signal is compared with the case of the signal with random phase. This complements the preceding works done by Yoshitani [9] and Helstrom [8] in terms of the numerical evaluation of the quantum Neyman-Pearson receiver for a binary thermal coherent state signal.

ACKNOWLEDGMENTS

The author is grateful to Professor Osamu Hirota of Tamagawa University for his helpful discussions. This work was supported in part by JSPS KAKENHI Grant Number 15K06082.

APPENDIX

The case of binary pure state detection was analytically solved by Helstrom [6]. This appendix is a short summary of his result.

To begin with, let us consider the following two pure states:

$$\mathsf{H}_0 : \hat{\rho}_0 = |\psi_0\rangle\langle\psi_0| \quad \text{and} \quad \mathsf{H}_1 : \hat{\rho}_1 = |\psi_1\rangle\langle\psi_1|, \quad (17)$$

where $\langle\psi_0|\psi_1\rangle = \kappa{\rm e}^{{\rm i}\theta}$, $0 < \kappa < 1$ and $0 \le \theta < 2\pi$. If $\alpha_0 = 0$, one can employ the Kennedy receiver [16] to construct the quantum NP receiver. It is given by

$$\hat{\Pi}_1 = \hat{1} - |\psi_0\rangle\langle\psi_0| \quad (18)$$

and hence

$$Q_{\rm d} = 1 - \kappa^2. \quad (19)$$

Here we let

$$\begin{aligned}|\mu_0\rangle &= r_{00}|\psi_0\rangle + r_{10}|\psi_1\rangle, \quad (20)\\ |\mu_1\rangle &= r_{01}|\psi_0\rangle + r_{11}|\psi_1\rangle, \quad (21)\end{aligned}$$

where

$$\begin{aligned}r_{00} &= \frac{1}{2}\left(\frac{1}{\sqrt{1+\kappa}} + \frac{1}{\sqrt{1-\kappa}}\right) = r_{11}, \quad (22)\\ r_{01} &= \frac{1}{2}\left(\frac{1}{\sqrt{1+\kappa}} - \frac{1}{\sqrt{1-\kappa}}\right){\rm e}^{{\rm i}\theta} = r_{10}^*. \quad (23)\end{aligned}$$

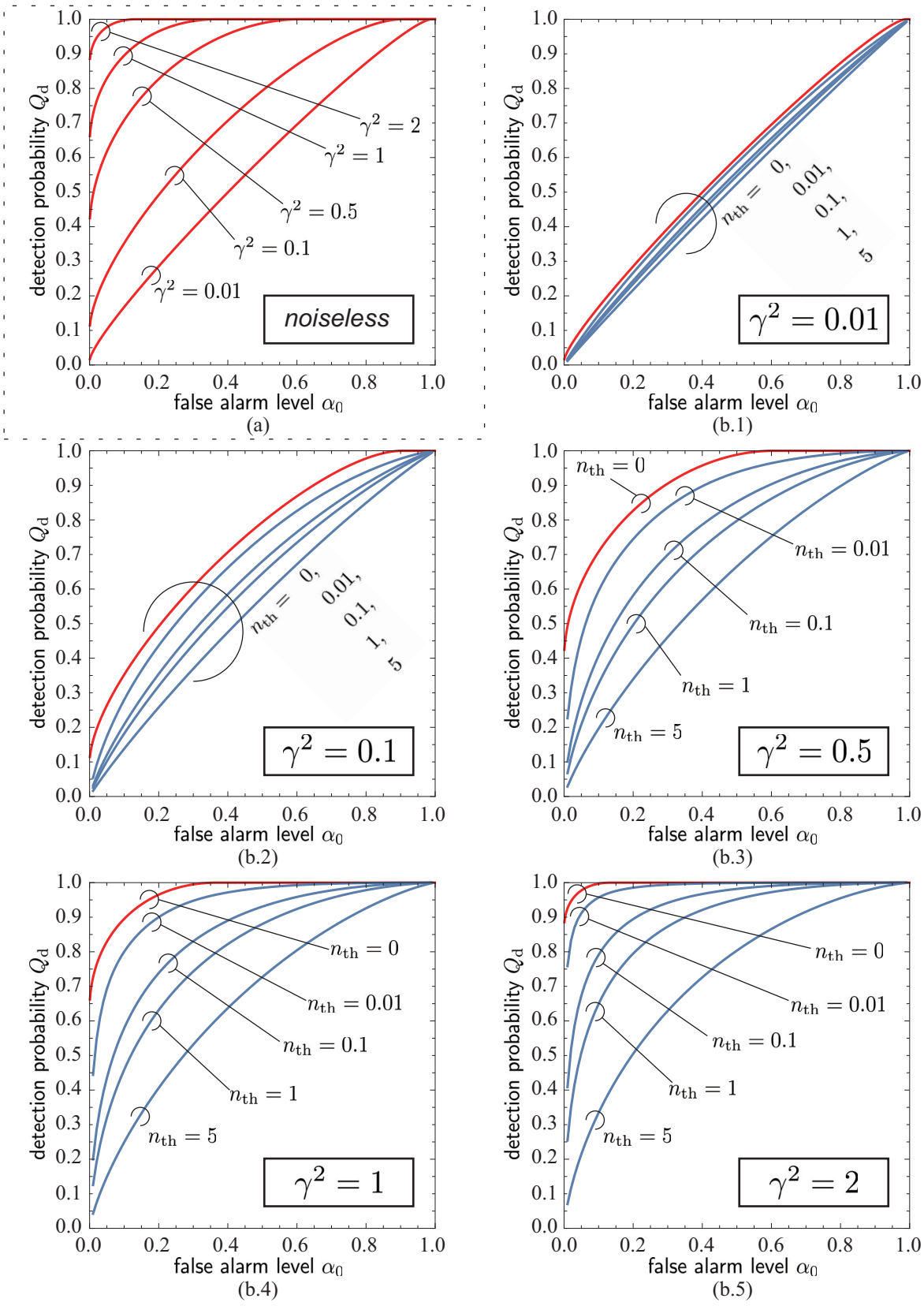

Fig. 1. Receiver operating characteristics (ROC) for binary coherent states in the presence of thermal noise. (a) noiseless cases ($\gamma^2 = 0.01, 0.1, 0.5, 1$ and 2). (b.1) case for $\gamma^2 = 0.01$ with thermal noise $n_{\rm th} = 0, 0.01, 0.1, 1$ and 5. (b.2) $\gamma^2 = 0.1$. (b.3) $\gamma^2 = 0.5$. (b.4) $\gamma^2 = 1$. (b.5) $\gamma^2 = 2$.

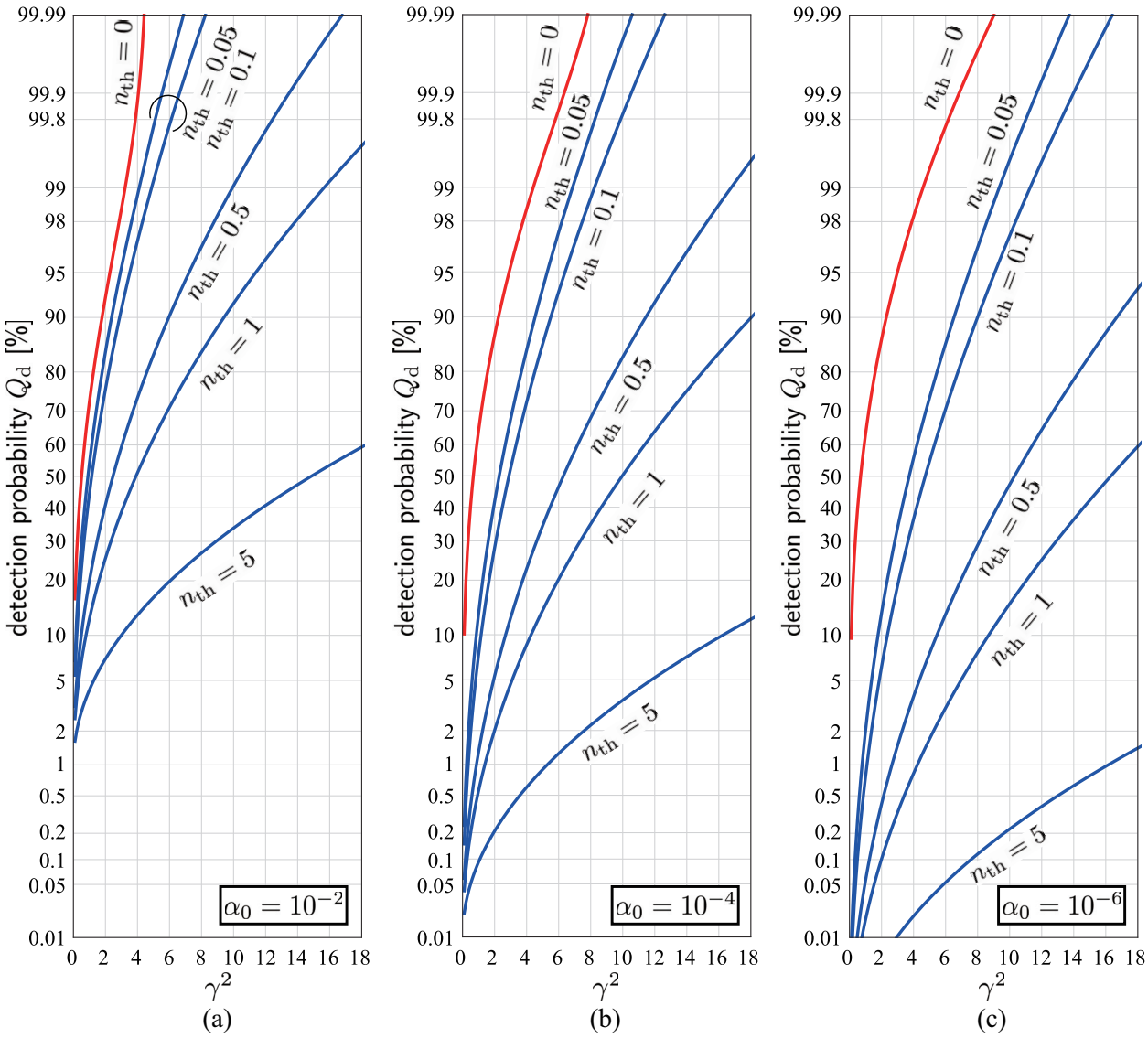

Fig. 2. Detection probability $Q_{\rm d}$ [%] versus γ^2. (a) $\alpha_0 = 10^{-2}$. (b) $\alpha_0 = 10^{-4}$. (c) $\alpha_0 = 10^{-6}$.

These vectors form an ordered orthonormal basis $\mathcal{B} = \{|\mu_0\rangle, |\mu_1\rangle\}$. Then the states $|\psi_0\rangle$ and $|\psi_1\rangle$ are rewritten as

$$\begin{aligned} |\psi_0\rangle &= s_{00}|\mu_0\rangle + s_{10}|\mu_1\rangle \\ &\doteq [|\psi_0\rangle]_{\mathcal{B}} = \begin{bmatrix} s_{00} \\ s_{10} \end{bmatrix}, \qquad (24) \\ |\psi_1\rangle &= s_{01}|\mu_0\rangle + s_{11}|\mu_1\rangle \\ &\doteq [|\psi_1\rangle]_{\mathcal{B}} = \begin{bmatrix} s_{01} \\ s_{11} \end{bmatrix}, \qquad (25) \end{aligned}$$

where

$$\begin{aligned} s_{00} &= \frac{1}{2}\left(\sqrt{1+\kappa} + \sqrt{1-\kappa}\right) = s_{11}, \qquad (26) \\ s_{01} &= \frac{1}{2}\left(\sqrt{1+\kappa} - \sqrt{1-\kappa}\right) \mathrm{e}^{\mathrm{i}\theta} = s_{10}^*. \qquad (27) \end{aligned}$$

Further, the matrix representations of $\hat{\rho}_0$ and $\hat{\rho}_1$ in the basis $\mathcal{B}$ are respectively given as follows.

$$\begin{aligned} \hat{\rho}_0 &\doteq [\hat{\rho}_0]_{\mathcal{B}} \\ &= \begin{bmatrix} \frac{1}{2}(1+\sqrt{1-\kappa^2}) & \frac{1}{2}\kappa \mathrm{e}^{\mathrm{i}\theta} \\ \frac{1}{2}\kappa \mathrm{e}^{-\mathrm{i}\theta} & \frac{1}{2}(1-\sqrt{1-\kappa^2}) \end{bmatrix}, \qquad (28) \end{aligned}$$

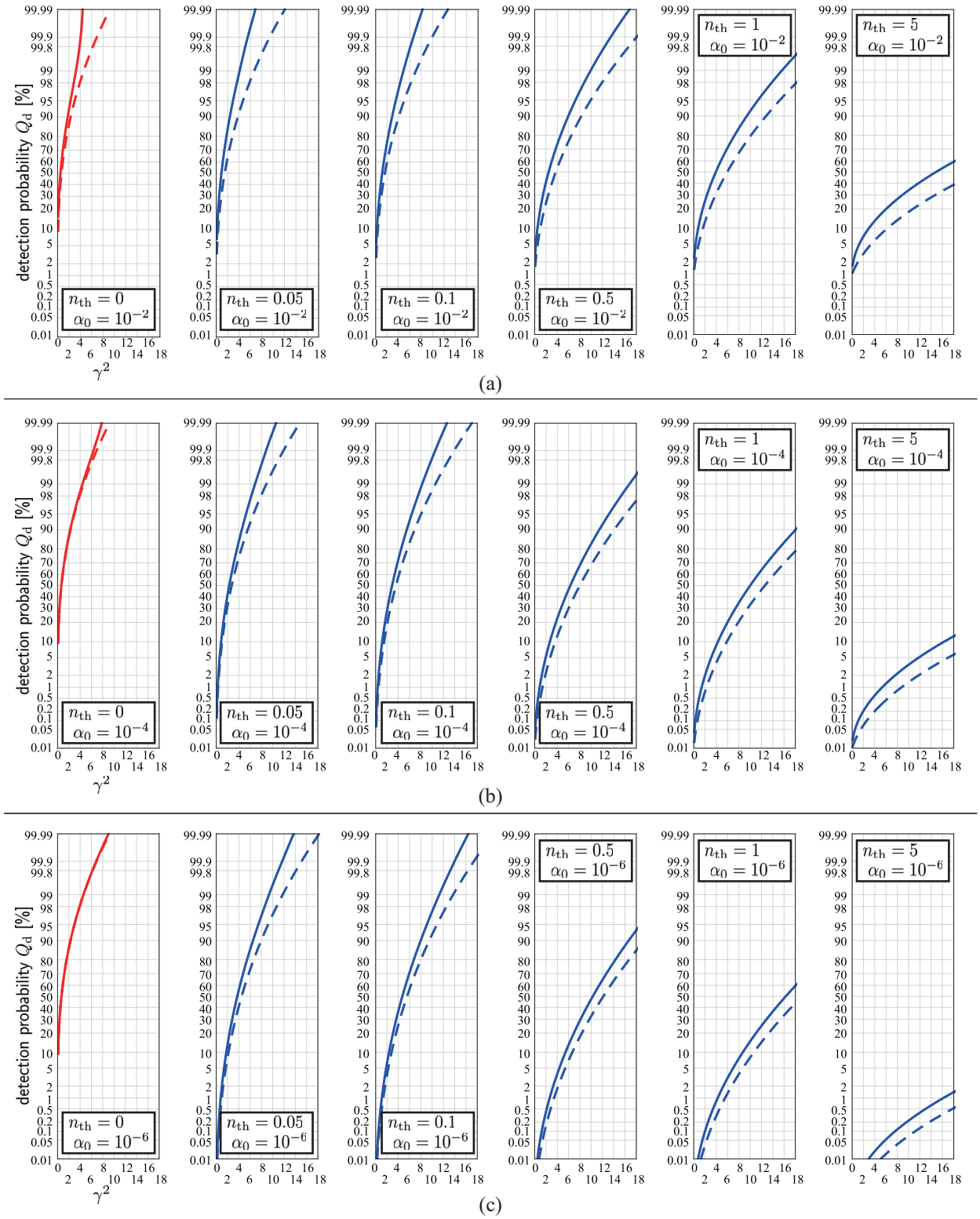

Fig. 3. Detection probability $Q_{\rm d}$ [%] for binary thermal coherent state signal of known phase and for that of unknown phase. Solid line: known phase cases. Dashed line: unknown phase cases. (a) $\alpha_0 = 10^{-2}$. (b) $\alpha_0 = 10^{-4}$. (c) $\alpha_0 = 10^{-6}$.

and

$$\begin{aligned}\hat{\rho}_1 &\doteq [\hat{\rho}_1]_{\mathcal{B}} \\ &= \begin{bmatrix} \frac{1}{2}(1-\sqrt{1-\kappa^2}) & \frac{1}{2}\kappa e^{i\theta} \\ \frac{1}{2}\kappa e^{-i\theta} & \frac{1}{2}(1+\sqrt{1-\kappa^2}) \end{bmatrix}. \quad (29)\end{aligned}$$

Hence we have

$$\hat{\rho}_1 - \zeta\hat{\rho}_0 \doteq [\hat{\rho}_1 - \zeta\hat{\rho}_0]_{\mathcal{B}} = \begin{bmatrix} A_{00} & A_{01} \\ A_{10} & A_{11} \end{bmatrix} \quad (30)$$

with

$$\begin{aligned}A_{00} &= \frac{1}{2}(1-\sqrt{1-\kappa^2}) - \frac{1}{2}(1+\sqrt{1-\kappa^2})\zeta, \quad (31)\\ A_{01} &= \frac{1}{2}\kappa e^{i\theta} - \frac{1}{2}\kappa\zeta e^{i\theta}, \quad (32)\\ A_{10} &= \frac{1}{2}\kappa e^{-i\theta} - \frac{1}{2}\kappa\zeta e^{-i\theta} = A_{01}^*, \quad (33)\\ A_{11} &= \frac{1}{2}(1+\sqrt{1-\kappa^2}) - \frac{1}{2}(1-\sqrt{1-\kappa^2})\zeta. \quad (34)\end{aligned}$$

From this one can find the eigenvalues of $\hat{\rho}_1 - \zeta\hat{\rho}_0$ as follows.

$$\begin{aligned}\lambda_- &= \frac{1}{2}(1-\zeta-\Lambda) < 0, \quad (35)\\ \lambda_+ &= \frac{1}{2}(1-\zeta+\Lambda) > 0, \quad (36)\end{aligned}$$

where $\Lambda = \sqrt{(1+\zeta)^2 - 4\zeta\kappa^2}$. The corresponding eigenvectors are then given by

$$\begin{aligned}|\lambda_-\rangle &= \hat{U}|\mu_0\rangle = u_{00}|\mu_0\rangle + u_{10}|\mu_1\rangle \\ &\doteq [|\lambda_-\rangle]_{\mathcal{B}} = \begin{bmatrix} u_{00} \\ u_{10} \end{bmatrix}, \quad (37)\\ |\lambda_+\rangle &= \hat{U}|\mu_1\rangle = u_{01}|\mu_0\rangle + u_{11}|\mu_1\rangle \\ &\doteq [|\lambda_+\rangle]_{\mathcal{B}} = \begin{bmatrix} u_{01} \\ u_{11} \end{bmatrix}, \quad (38)\end{aligned}$$

where we have defined

$$\begin{aligned}\hat{U} &= u_{00}|\mu_0\rangle\langle\mu_0| + u_{01}|\mu_0\rangle\langle\mu_1| \\ &\quad + u_{10}|\mu_1\rangle\langle\mu_0| + u_{11}|\mu_1\rangle\langle\mu_1|, \\ &\doteq [\hat{U}]_{\mathcal{B}} = \begin{bmatrix} u_{00} & u_{01} \\ u_{10} & u_{11} \end{bmatrix} \quad (39)\end{aligned}$$

with

$$\begin{aligned}u_{00} &= \frac{\Lambda + (1+\zeta)\sqrt{1-\kappa^2}}{\sqrt{2\Lambda^2 + 2(1+\zeta)\Lambda\sqrt{1-\kappa^2}}} = u_{11}, \quad (40)\\ u_{01} &= \frac{\kappa(1-\zeta)e^{i\theta}}{\sqrt{2\Lambda^2 + 2(1+\zeta)\Lambda\sqrt{1-\kappa^2}}} = -u_{10}^*. \quad (41)\end{aligned}$$

Letting

$$\begin{aligned}\hat{\Pi}_0 &= |\lambda_-\rangle\langle\lambda_-| = \hat{U}|\mu_0\rangle\langle\mu_0|\hat{U}^\dagger, \\ &\doteq [\hat{\Pi}_0]_{\mathcal{B}} \\ &= \begin{bmatrix} 1 - \frac{1}{\Omega}(1-\zeta)^2\kappa^2 & -\frac{1}{2\Lambda}(1-\zeta)\kappa e^{i\theta} \\ -\frac{1}{2\Lambda}(1-\zeta)\kappa e^{-i\theta} & \frac{1}{\Omega}(1-\zeta)^2\kappa^2 \end{bmatrix} \quad (42)\end{aligned}$$

and

$$\begin{aligned}\hat{\Pi}_1 &= |\lambda_+\rangle\langle\lambda_+| = \hat{U}|\mu_1\rangle\langle\mu_1|\hat{U}^\dagger \\ &\doteq [\hat{\Pi}_1]_{\mathcal{B}} \\ &= \begin{bmatrix} \frac{1}{\Omega}(1-\zeta)^2\kappa^2 & \frac{1}{2\Lambda}(1-\zeta)\kappa e^{i\theta} \\ \frac{1}{2\Lambda}(1-\zeta)\kappa e^{-i\theta} & 1 - \frac{1}{\Omega}(1-\zeta)^2\kappa^2 \end{bmatrix} \quad (43)\end{aligned}$$

with $\Omega = 2\Lambda\left\{\Lambda + (1+\zeta)\sqrt{1-\kappa^2}\right\}$, the type-I error probability $\alpha(\zeta) = P(1|0)$ and the type-II error probability $\beta(\zeta) = P(0|1)$ are respectively given by

$$\begin{aligned}\alpha(\zeta) &= \frac{1}{2} - \frac{(1+\zeta) - 2\kappa^2}{2\Lambda}, \quad (44)\\ \beta(\zeta) &= \frac{1}{2} - \frac{(1+\zeta) - 2\zeta\kappa^2}{2\Lambda}. \quad (45)\end{aligned}$$

A typical behavior of $\alpha(\zeta)$ and $\beta(\zeta)$ is illustrated in

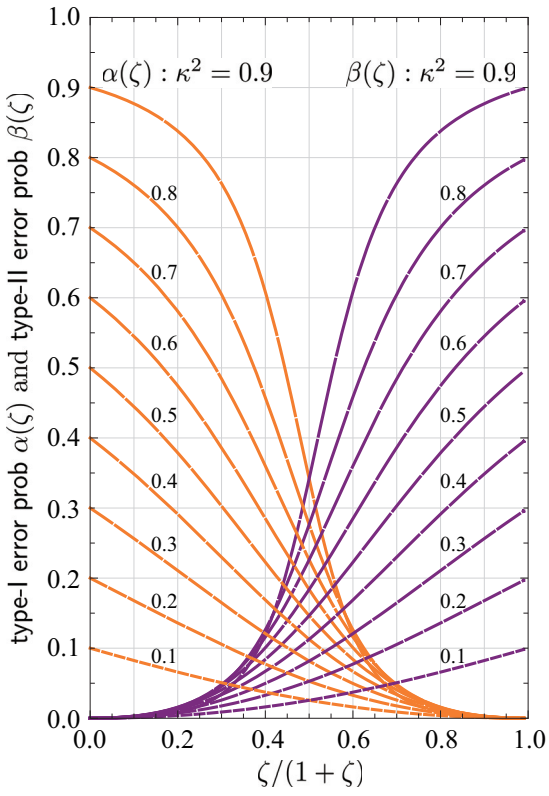

Fig. 4. $\alpha(\zeta)$ and $\beta(\zeta)$.

Fig. 4. Form this we observe there is a trade-off relation between $\alpha(\zeta)$ and $\beta(\zeta)$ for the choice of ζ.

The remaining task for the the NP criterion is to find the optimal ζ that maximizes the detection probability $1-\beta(\zeta)$ under the constraint $\alpha(\zeta) \le \alpha_0$. When α_0 is chosen as $\kappa^2 < \alpha_0 \le 1$, the constraint $\alpha(\zeta) \le \alpha_0$ can be replaced to $\alpha(\zeta) = \kappa^2$ since the maximum value of $\alpha(\zeta)$ is κ^2 and there is a trade off relation between $\alpha(\zeta)$ and $\beta(\zeta)$. Solving the equation $\alpha(\zeta) = \kappa^2$, the optimal ζ° is 0. When α_0 is chosen as $0 < \alpha_0 \le \kappa^2$, then the constraint

$\alpha(\zeta) \leq \alpha_0$ can be replaced to $\alpha(\zeta) = \alpha_0$. Solving the equation $\alpha(\zeta) = \alpha_0$, we have

$$\zeta^\circ = -(1-2\kappa^2) + (1-2\alpha_0)\sqrt{\frac{(1-\kappa^2)\kappa^2}{(1-\alpha_0)\alpha_0}},$$

where we have used the condition $\zeta > 0$. Substituting the optimal ζ° into Eq.(45), we have

$$\begin{aligned} Q_{\rm d} &= 1 - \beta(\zeta^\circ) \\ &= \begin{cases} 1-\kappa^2, & \text{if } \alpha_0 = 0; \\ \left(\kappa\sqrt{\alpha_0} + \sqrt{(1-\alpha_0)(1-\kappa^2)}\right)^2, & \\ & \text{if } 0 < \alpha_0 \leq \kappa^2; \\ 1, & \text{if } \kappa^2 < \alpha_0 \leq 1. \end{cases} \end{aligned} \tag{46}$$

Thus we could reach to the result shown in Eq.(2.33) of the textbook [10] (or Eq.(2.18) of the literature [8]).

At the tail of this appendix, we must mention that the analysis above is mainly based on the analysis used in the literature [17] which treats the problem of the minimax criterion. In this analysis we have used a technique of the square-root measurement.

REFERENCES

[1] J. Neyman and E. S. Pearson, "On the Problem of the most Efficient Tests of Statistical Hypotheses," Phil. Trans. R. Soc. Lond. A, vol.A231, no.9, pp.289-337, 1933.

[2] J. Neyman and E. S. Pearson, "The testing of statistical hypotheses in relation to probabilities a priori," Proc. Camb. Philos. Soc., vol.29, no.4, pp.492-510, 1933.

[3] H. V. Hance, "The optimization and analysis of systems for the detection of pulse signals in random noise," Sc.D. dissertation, M.I.T., Jan. 2, 1951.

[4] D. Middleton, "Statistical Criteria for the Detection of Pulsed Carriers in Noise. I," J. Appl. Phys., vol.24, no.4, pp.371-378, 1953; D. Middleton, "Statistical Criteria for the Detection of Pulsed Carriers in Noise. II," J. Appl. Phys., vol.24, no.4, pp.379-391, 1953.

[5] M. A. Richards, Fundamentals of Radar Signal Processing, McGraw-Hill, New York, 2005.

[6] C. W. Helstrom, "Detection Theory and Quantum Mechanics," Inform. Contr., vol.10, no.3, pp.254-291, 1967; C. W. Helstrom, "Detection Theory and Quantum Mechanics (II)," Inform. Contr., vol.13, no.2, pp.156-171, 1968.

[7] C. W. Helstrom, "Performance of an Ideal Quantum Receiver of a Coherent Signal of Random Phase," IEEE Trans. Aerosp. Electron. Syst., vol.AES-5, no.3, pp.562-564, 1969.

[8] C. W. Helstrom, "Quantum Detection Theory," Progress in Optics, pp.289-369, 1972.

[9] R. Yoshitani, "On the Detectability Limit of Coherent Optical Signals in Thermal Radiation," J. Stat. Phys., vol.2, no.4, pp.347-378, 1970.

[10] C. W. Helstrom, Quantum Detection and Estimation Theory, Academic Press, New York, 1976.

[11] B. R. Mollow and R. J. Glauber, "Quantum Theory of Parametric Amplification. I," Phys. Rev., vol.160, no.5, pp.1076-1096, 1967.

[12] M. Abramowitz and I. A. Stegun, Ed., Handbook of Mathematical Functions With Formulas, Graphs, and Mathematical Tables, Applied Mathematics Series 55, National Bureau of Standards, United States Department of Commerce, Washington, D.C., 1964.

[13] C. W. Helstrom, "Bayes-Cost Reduction Algorithm in Quantum Hypothesis Testing," IEEE Trans. Inform. Theory, vol.IT-28, no.2, 1982.

[14] GSL - GNU Scientific Library. http://www.gnu.org/software/gsl/

[15] G. Lachs, "Theoretical Aspects of Mixtures of Thermal and Coherent Radiation," Phys. Rev., vol.138, no.4B, pp.B1012-B1016, 1965.

[16] R. S. Kennedy, "A near-optimum receiver for the binary coherent state quantum channel," M.I.T. Res. Lab. Electron. Quart. Progr. Rep., vol.110, pp.142-146, 1973.

[17] K. Kato, "Necessary and Sufficient Conditions for Minimax Strategy in Quantum Signal Detection," Proc. IEEE ISIT 2012, pp.1077-1081, 2012.